J Electroceram (2011) 27:24–28
DOI 10.1007/s10832-010-9610-y

High performance thin film PZT ultrasonic transducer by CSD for distance measurements in water

E. Heinonen · J. Juuti · J. Palosaari · F. Tyholdt · H. Jantunen · N. P. Østbø · A. Vogl · E. Poppe · S. Guðbjörnsson · E. Ringgaard · B. Hök · P.-E. Fägerman · P. Gløersen · H. Ræder

Received: 21 September 2008 / Accepted: 20 April 2010 / Published online: 8 May 2010

Abstract Piezoelectric thin film ultrasonic transducers were realised and tested for short range distance measurements. Displacements in air and water as a function of frequency were modelled by Comsol Multiphysics finite element modelling (FEM) and transducer configurations with a two electrode layout were manufactured to enable larger displacements than with the conventional design. The transducer was fabricated on a silicon wafer by chemical solution deposition (CSD) with total PZT ($Pb(Zr_{0.53}Ti_{0.47})O_3$) thickness of 2 µm. Subsequently, a cavity underneath the PZT was wet etched creating a bending membrane with a total thickness of ~13 µm. The displacements of the transducers as a function of frequency were modelled and measured by fiber-optic laser vibrometer. The effective piezoelectric d_{33} coefficient of 300 nm/V and 144 nm/V in air and 48 nm/V and 18 nm/V in water was obtained for 260×260 µm^2 and 390×390 µm^2 membranes, respectively. The accuracy of the modelled resonance frequencies both in air and water was relatively good, of ~4-13% and ~5-20%, respectively.

Keywords Piezoelectric · Ultrasonic · Transducer · FEM · CSD

1 Introduction

Mass-producible silicon based MEMS (micro-electromechanical systems) have been exploited in various fields of industry, for example in telecommunication, automotive and electronics. The most commonly used mechanism to create force and displacement in MEMS is based on the electrostatics which, however, is quite limited in terms of speed, force and energy efficiency. To overcome this

E. Heinonen (✉) · J. Juuti · J. Palosaari · H. Jantunen
Microelectronics and Materials Physics Laboratories,
EMPART Research Group of Infotech, University of Oulu,
OuluP.O.Box 4500, Fin-90014, Finland
e-mail: Esa.Heinonen@ee.oulu.fi

F. Tyholdt · N. P. Østbø · A. Vogl · E. Poppe
SINTEF,
P.O. Box 124, Blindern,
NO-0349 Oslo, Norway

S. Guðbjörnsson
Star-Oddi Ltd,
Vatnagardar 14,
104 Reykjavik, Iceland

E. Ringgaard
InSensor A/S,
Hejreskovvej 18A,
DK-3490 Kvistgård, Denmark

B. Hök
Hök Instrument AB,
Flottiljgatan 49,
SE-721 31 Västerås, Sweden

P.-E. Fägerman
Mandalon Technologies AB,
Westmansgatan 49,
582 16 Linköping, Sweden

P. Gløersen
Infineon Technologies SensoNor AS,
Knudsrødveien 7, P.O. Box 196, 3192 Horten, Norway

H. Ræder
Sonitor Technologies AS,
Forskningsveien 1B,
NO-0373 Oslo, Norway

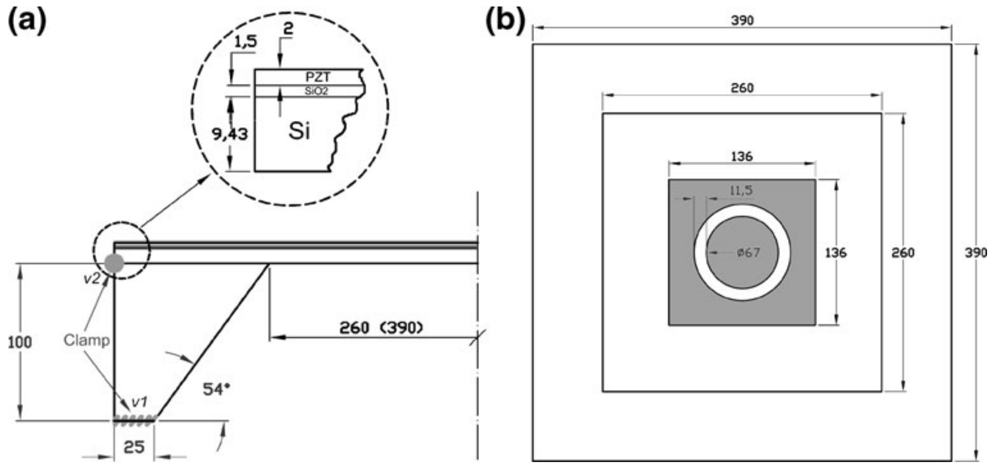

Fig. 1 The transducer structure; **(a)** cross-section and **(b)** the two electrode design (*grey*), dimensions in μm

problem many other mechanisms have been developed like magnetic, thermal and piezoelectric actuation. Especially silicon based thin film piezoelectrics have shown promising properties to be utilised in a wide variety of novel applications like accelerometers, ultrasonic transducers, pressure and flow sensors, micromotors, micropumps, and microsensors for different purposes. [1] High performance silicon based piezoelectric MEMS devices enables innovative applications like fish tags, in this case, for biological research to study behaviour and internal organs of the fishes in their natural environment [2, 3]. In such application, compact size, low cost, long-term reliability in harsh conditions and low power consumption are necessities. In this paper, thin film piezoelectric ultrasonic transducers with a two electrode configuration processed via chemical solution deposition (CSD) on a silicon wafer are introduced and their in air and in water characteristics are modelled and measured.

2 Experimental

The transducer was fabricated on a silicon wafer by CSD where 32 sequential layers of PZT ($Pb(Zr_{0.53}Ti_{0.47})O_3$) were deposited with the total thickness of 2 μm [4]. Subsequently, a cavity underneath the piezoelectric layer was wet etched creating a bending membrane with a total thickness of ~13 μm. A gold top electrode, platinum bottom electrode, SiO_2 and Si layers under the PZT were 0.15 μm, 0.12 μm, 1.5 μm and 9.43 μm thick, respectively. Two different transducers with cavity sizes of 260×260 μm^2 and 390×390 μm^2 were modelled and measured. The inner electrode in both transducers was 67 μm in diameter and the width of the square shaped outer electrode was 136 μm. The insulation gap between the two electrodes was 11.5 μm. The layer thicknesses and geometry of the modelled structures can be seen in Fig. 1(a) and (b).

The working principle of the two electrode design is presented in Fig. 2. According to the earlier modelling experience, the displacement behavior of the transducer with the two electrode layout was better compared to a conventional electrode with the same area, e.g. in this case to a round electrode with a diameter of ~141 μm or to a square electrode of ~125×125 μm^2.

The ultrasonic transducer was poled with a 10 V/μm electric field at 100°C temperature. The displacement as a function of frequency in the centre of the transducer was measured using fibre-optic laser vibrometer OFV-5000 (Polytec GmbH, Germany) and XY-table [5–7] with 1.25

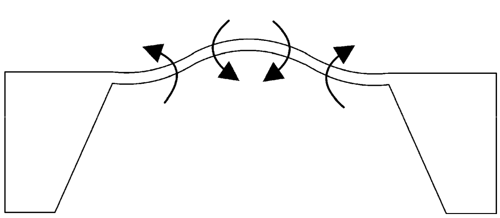

Fig. 2 Working principle of the two electrode design

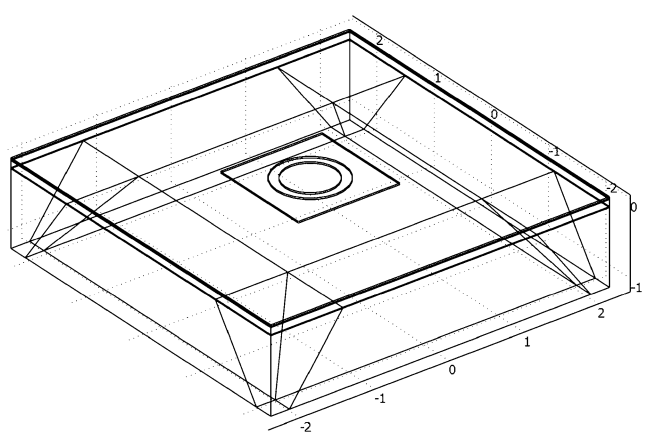

Fig. 3 The 3D model of the transducer structure

Table 1 Material parameters used in the FEM models.

Material	Elastic compliance coefficients (× $10^{-12} m^2/N$)						
	s_{11}	s_{12}	s_{13}	s_{33}	s_{44}	s_{66}	
PZT	9.09	-2.55	-5.75	16.00	33.30	32.79	
	Density (kg/m^3)		Piezoelectric coefficients (pm/V)			Relative permittivity	
			d_{31}	d_{33}	d_{15}	$\varepsilon_{11}/\varepsilon_0$	$\varepsilon_{33}/\varepsilon_0$ (K_{33})
PZT	7750		-165	85	496	1475	1300
	Density (kg/m^3)	Young's Modulus (GPa)				Poisson's ratio	
Si	2330	166				0.278	
SiO_2	2200	70				0.30	

and 2.5 V/μm electric fields. Comsol Multiphysics finite element modelling (FEM) software version 3.4 was used in the modelling of the transducers. Both in air and in water models were calculated. In the modelling, the 2D wireframe (Fig. 1) was first done using AutoCAD2002 and then imported into Comsol Multiphysics where it was processed into a 3D model seen in Fig. 3.

The top and bottom electrode layers of the transducer were not modelled as the earlier experience indicated that they have a very small effect to the results. Furthermore, meshing of the very thin layers increases the calculation times and the computer memory requirements, and can also introduce resolving and accuracy problems in the FEM software due to the aspect ratios. Instead, the electrode patterns shown in Fig. 1(b) were modelled as “face” layers (Fig. 3). Two different clamping conditions were used and their effect to the displacement behaviour was studied. In the first clamping condition, *v1*, the clamp was introduced along the bottom surfaces and in the second clamping condition, *v2*, along the side lines of the transducer structure, as shown in Fig. 1(a). Structural damping with loss factors of 0.03 and 0.01 were used in the models for all solid materials. The density and speed of sound were set to 1.25 kg/m^3 and 343 m/s in the air and to 1000 kg/m^3 and 1500 m/s in the water, respectively. The material parameters of the solid materials used in the modelling are shown in Table 1 [4, 8].

3 Results and discussion

The modelling and measurement results of the transducers in air and in water with the 260×260 μm^2 and 390×390 μm^2 cavities and with different clamping conditions and loss factors can be seen in Figs. 4 and 5. Electric fields of 1.25 V/μm were used, except for the transducer in water with the 390×390 μm^2 cavity, where electric field of 2.5 V/μm was used in order to get a sufficient response from the measurements. In the modelling, decreased loss, i.e. increased Q factor, introduced

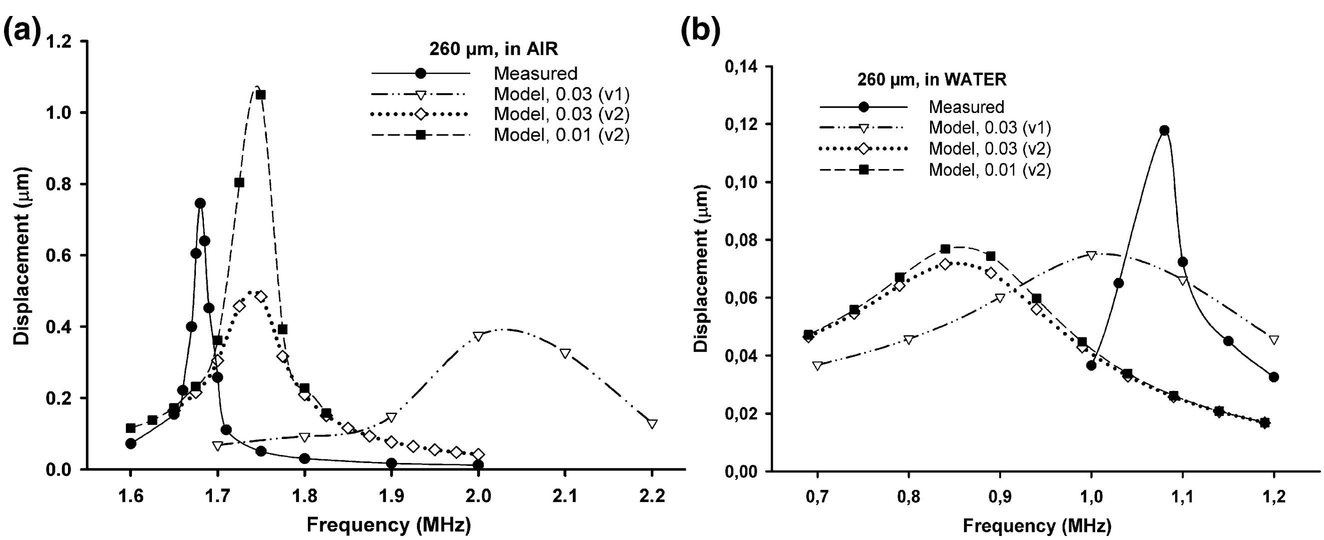

Fig. 4 Measured and modelled displacements as a function of frequency of the 260×260 μm^2 cavity transducer, **(a)** in air and **(b)** in water with 1.25 V/μm

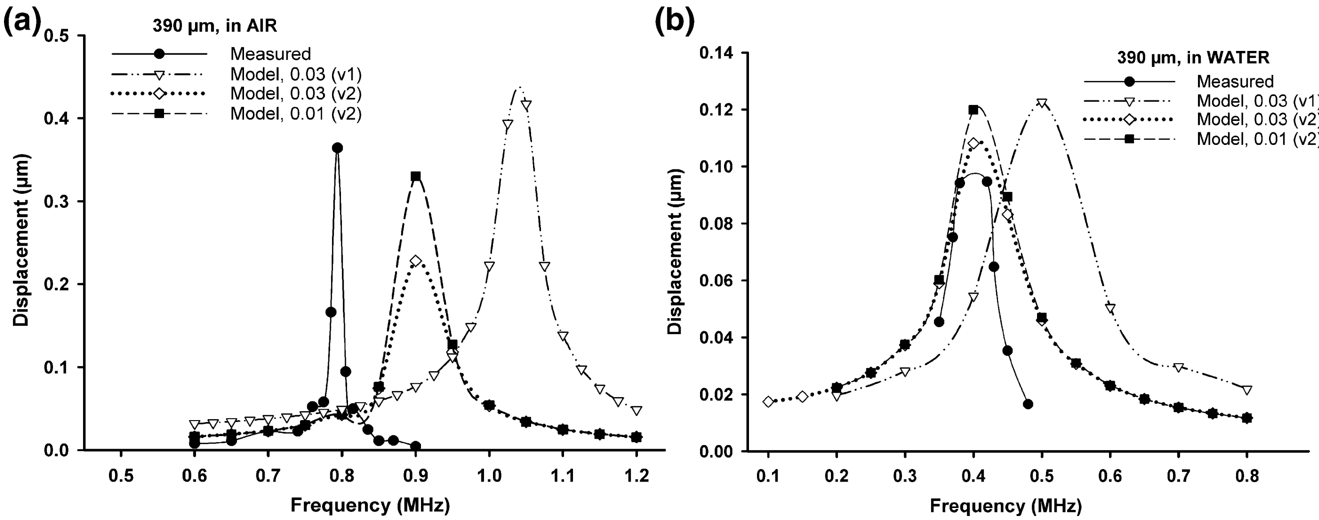

Fig. 5 Measured and modelled displacements as a function of frequency of the 390×390 μm^2 cavity transducer, **(a)** in air with 1.25 V/μm and **(b)** in water with 2.5 V/μm

larger displacements near the resonance while the displacements were about the same at frequencies off the resonance, as can be expected. The in water resonance frequencies shifts down because the water creates a load to the structure. Besides this, only the clamping conditions had an effect on the resonance frequencies. That is, the tighter clamping of case *v1* (bottom surface clamp, Fig. 1) stiffens the structure, thus increasing the resonance frequencies. It should be noted, that in the clamping case *v2* (side lines clamp, Fig. 1) the deflection of the cavity sidewalls are allowed while in the case of *v1* such deformation is greatly reduced. This behaviour corresponds relatively well to the measurement conditions (transducers were measured in a matrix, and clamped from the edges allowing horizontal deformations). Also, in all cases, excluding the 260×260 μm^2 cavity transducer in water, the *v2* clamping condition modelling results are closer to the experimental curves and can be considered as a better option to be used in the FEM. The anomalous resonance behaviour of the 260×260 μm^2 cavity transducer in water requires further experiments which will be conducted in the future.

The measured resonance displacements of the transducers in air were ~0.75 μm and ~0.36 μm or 300 nm/V and 144 nm/V with cavity sizes of 260×260 μm^2 and 390×390 μm^2, respectively. The in water displacements were reduced to ~0.12 μm and ~0.09 μm or to 48 nm/V and 18 nm/V, respectively. The in air results compared relatively well to the deflection of 400 nm/V of a 140 μm in diameter and 4 μm thick PZT transducer cell reported by Muralt et al. [13]. However, the measured in water deflections were considerably higher compared to the reported value of 2 nm/V. One possible reason for this could be the two electrode layout; however, this requires further experiments which will be performed in the future.

According to the previous studies by Heinonen et al. [9–11] and Duval et al. [12], the accuracy of the piezoelectric models decreased with higher (>1 V/μm) electric fields, mainly because non-linear characteristics are typical for the piezoelectric materials at higher voltages. As shown in Figs. 4 and 5, the modelling accuracy with the bottom surface clamp *v1* of the in air and in water resonance frequencies were ~19-32% and ~7-19%, respectively. With the side lines clamp *v2*, the accuracy of the in air and in water models were ~4-13% and ~5-20%, respectively. The accuracy can be considered relatively good, since for example in [9, 11] accuracies of ~10% were reported with lower electric fields (< 1 V/μm) and well known conditions. Many aspects such as clamping conditions and material parameters affect to the modelling. In the MEMS devices the aspect ratios, i.e. the thin layers, propose an additional challenge. Further parameter verification and characterization of the structure is required to improve the accuracy of the modelling which will be performed in the future.

4 Conclusions

The accuracy of the modelled in air and in water resonance frequencies remained relatively good, of ~4-13% and ~5-20%, respectively (with electric fields of 1.25 V/μm and 2.5 V/μm). The loss factor affected to the displacements dramatically near the resonance, thus more characterization is required to improve the modelling results. Moreover, to improve the accuracy of the modelling, knowledge of the other material parameters, boundary conditions and the exact geometry are all very critical aspects.

Acknowledgements The authors acknowledge the support of the Nord-Pie project funded by Nordic Innovation Centre. Author J. Juuti also acknowledges the Hi-piezo project funded by Academy of Finland (project number 124011).

References

1. H. Ræder, F. Tyholdt, W. Booij, F. Calame, N.P. Østbø, R. Bredesen, K. Prume, G. Rijnders, P. Muralt, J Electroceram **19**, 357 (2007)
2. O.R. Godø, K. Michalsen, Fish Res **48**, 127 (2000)
3. T. Sigurdsson, V. Thorsteinsson, L. Gústafsson, ICES J Mar Sci **63**, 523 (2006)
4. F. Tyholdt, F. Calame, K. Prume, H. Ræder, P. Muralt, J Electroceram **19**(4), 311 (2007)
5. Z. Huang, G. Leighton, R. Wright, F. Duval, H.C. Chung, P. Kirby, R.W. Whatmore, Sens. Actuators A-Phys. **135**(2), 660 (2006)
6. K. Yao, F.E.H. Tay, IEEE Trans Ultrason Ferroelectr Freq Control **50**(2)), 113 (2003)
7. J. Palosaari, J. Juuti, E. Heinonen, V.-P. Moilanen, H. Jantunen, Journal of Electroceramics. (2008) doi:10.1007/s10832-008-9440-3.
8. P. Muralt, N. Ledermann, J. Baborowski, A. Barzegar, S. Gentil, B. Belgacem, S. Petitgrand, A. Bosseboeuf, N. Setter, IEEE Trans Ultrason Ferroelectr Freq Control **52**(12), 2276 (2005)
9. E. Heinonen, J. Juuti, S. Leppävuori, J. Eur. Ceram. Soc. **25**(12), 2467 (2005)
10. E. Heinonen, J. Juuti, H. Jantunen, J. Eur. Ceram. Soc **25**(12), 2467 (2007)
11. E. Heinonen, J. Juuti, V.-P. Moilanen, J. Palosaari, H. Jantunen, Journal of Intelligent Material Systems and Structures. (2008) doi:10.1177/1045389X08097384.
12. F. Duval, S. Wilson, G. Ensell, N. Evanno, M. Cain, R. Whatmore, Sensors and Actuators A **133**(1), 35 (2007)
13. P. Muralt, D. Schmitt, N. Ledermann, J. Baborowski, P.K. Weber, W. Steichen, S. Petitgrand, A. Bosseboeuf, N. Setter, P. Gaucher, IEEE Ultrasonics Symposium **2**, 907 (2001)